

Conical Intersection Pathways in the Photocycloaddition of Ethene and Benzene: A CASSCF Study with MMVB Dynamics

Simon Clifford,[†] Michael J. Bearpark,[†] Fernando Bernardi,[§] Massimo Olivucci,^{*,§} Michael A. Robb,^{*,†} and Barry R. Smith[†]

Contribution from the Department of Chemistry, King's College London, Strand, London, WC2R 2LS, UK, and Dipartimento di Chimica "G. Ciamician" dell' Università di Bologna, Via Selmi 2, 40126 Bologna, Italy

Received April 1, 1996. Revised Manuscript Received June 4, 1996[⊗]

Abstract: Pathways involving possible conical intersections and radicaloid intermediates on the potential energy surface for the photocycloaddition of ethene to benzene have been studied using CASSCF geometry optimization and MMVB simulation of conical intersection decay dynamics. This study is intended as a model for arene–alkene photochemistry. The formation of one C–C bond occurs without barrier to yield a low energy conical intersection. Whilst many of the previously postulated intermediates do exist, the reactivity is shown to be controlled by this single conical intersection that has the geometry of a distorted tetrahedron with 4 carbon centers at its vertices. Such a structure is similar to the one encountered in the sigmatropic migration of the methyl group in but-1-ene and of the allyl group in hexa-1,5-diene. The dynamics of the decay at this conical intersection, studied with MMVB, show that one may form either the *ortho*, *meta*, or *para* products. However, ground state relaxation valleys have been located for the *meta* and *ortho* products only. This is consistent with experiment in solution where *ortho* and *meta* products are formed with approximately equal quantum yields.

Introduction

The photocycloaddition reactions of arenes with alkenes are theoretically intriguing because the mechanistic preference to form the three cycloaddition products (Figure 1) is poorly rationalized by the usual orbital symmetry correlations. These reactions also have considerable synthetic potential (see refs 1 and 2 for comprehensive reviews), yet, to date, only very limited theoretical work along assumed reaction paths has been reported. In this paper we report a study of the model reaction of benzene and ethene.³ Our objective is to understand the topology of this S_1 potential energy surface and thus to determine the role of the various intermediate structures that have been postulated to rationalize experimental observations.

With many arene + olefin systems one or both of the 1,2- and 1,3-cycloadditions proceed with good yields, whereas the 1,4-addition is a less efficient process preferred only in a few special cases. In the case of the model system, ethene adds to benzene forming primarily the *meta* adduct ($\phi = 0.11$, 50 bar, 12 mol/L ethene + 1 M benzene in dichloromethane), and other products ($\phi = 0.08$) most of which are either the *ortho* product or its photoproducts.³ The quantum yield is measured relative to the benzene fluorescence. In Scheme 1, we have illustrated some plausible intermediate structures that may occur along the possible reaction pathways. Some of these structures have been postulated experimentally, while others are suggested by theoretical considerations that we shall discuss subsequently. Experimentally, a charge transfer adduct (**II** in Scheme 1) has been invoked for the 1,2-pathway because the *ortho* adduct is

often favored when the alkene is a better electron donor or electron acceptor than the arene (but there is no direct experimental evidence). Thus the substituted *ortho* (and *para*) addition intermediates may be polarized (**II** in Scheme 1) and are therefore stabilized by charge transfer.^{4,5} This has led to empirical rules^{6–8} to determine the mode of addition by the difference in electron donor characteristics: *meta* addition is favored for low difference reactants; *ortho* otherwise; and *para* in a very few cases where there are other important considerations, such as steric factors. The *meta* addition is also often postulated to involve a biradical intermediate (**III** on S_1). Since the stereochemistry of the ethene fragment is usually preserved, the additions are considered to be concerted. Thus the bonds between the alkene and the benzene must be formed nearly simultaneously. The closure of the three-membered ring may occur in the next stage of the reaction, via a radical or in a concerted, nonsynchronous fashion.

The mechanisms of all three additions have been discussed in terms of orbital symmetry rules,^{9,1,5} despite the unsuitability of these rules for aromatic rings due to the degeneracy of the molecular orbitals in aromatic systems and the fact that a constant plane of symmetry in the system must be assumed throughout the reaction. Houk has used a frontier orbital overlap method to describe the reaction,⁴ which assumes that the wave function of the system is well described by MO theory. Van

(4) Houk, K. N. *Pure Appl. Chem.* **1982**, *54*, 1673.

(5) Bryce-Smith, D. *Pure Appl. Chem.* **1973**, *34*, 193.

(6) Bryce-Smith, D.; Gilbert, A.; Orger, B. H.; Tyrrell, H. J. *Chem. Soc., Chem. Commun.* **1974**, 334.

(7) Gilbert, A.; Yianni, P. *Tetrahedron* **1981**, *37*, 3275.

(8) Mattay, J. *Tetrahedron* **1985**, *41*, 2405.

(9) Bryce-Smith, D. *J. Chem. Soc., Chem. Commun.* **1969**, 806.

(10) (a) Van der Hart, J. A.; Mulder, J. J. C.; Cornelisse, J. J. *Mol. Struct. (Theochem)* **1987**, *151*, 1. (b) Van der Hart, J. A.; Mulder, J. J. C.; Cornelisse, J. J. *Photochem. Photobiol., A: Chem.* **1991**, *61*, 3. (c) Stehouwer, A. M.; Van der Hart, J. A.; Mulder, J. J. C.; Cornelisse, J. J. *Mol. Struct. (Theochem)* **1992**, *92*, 333. (d) Van der Hart, J. A.; Mulder, J. J. C.; Cornelisse, J. J. *Photochem. Photobiol., A: Chem.* **1995**, *86*, 141.

[†] King's College London.

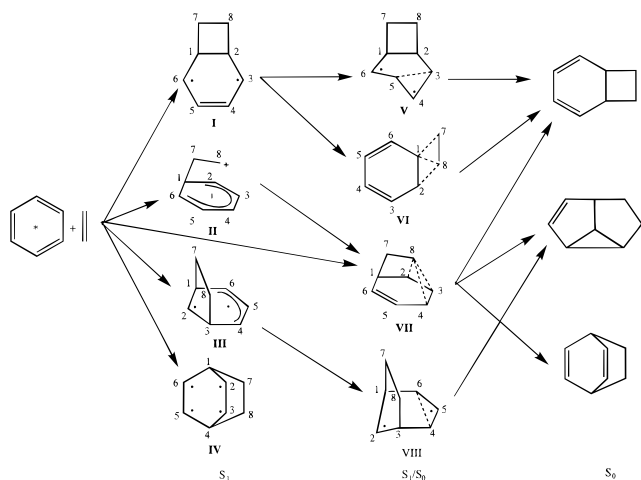
[§] "G. Ciamician" dell' Università di Bologna.

[⊗] Abstract published in *Advance ACS Abstracts*, July 15, 1996.

(1) Bryce-Smith, D.; Gilbert, A. *Tetrahedron* **1976**, *32*, 1309; **1977**, *33*, 2459.

(2) Cornelisse, J. J. *Chem. Rev.* **1993**, *93*, 615–669.

(3) Mirbach, M. F.; Mirbach, M. J.; Saus, A. *Tetrahedron. Lett.* **1977**, 959.

Scheme 1. Predicted Structures for the Model Benzene + Ethene Reaction Pathways

der Hart, Cornelisse, and co-workers¹⁰ have studied the reaction using semiempirical and *ab initio* methods (but without full geometry optimization) as well as by orbital symmetry correlations. Their work suggests that surface crossings can occur on the ortho and meta reaction paths. All the experiments and theoretical studies suggest that the excited species is S_1 benzene (the wavelength of light used, 254 nm, corresponds to the $S_0 \rightarrow S_1$ transition in benzene). For a complete review see ref 2.

In this paper we shall argue that the existence of intermediates and surface crossings on the model (ethene + benzene) olefin + arene photoaddition reaction surface can be easily predicted with a simple VB model.^{11a} These intermediates and surface crossings have been optimized at the CASSCF level. Only one of these points (VII in Scheme 1) appears to be energetically accessible for the model reaction and corresponds to a conical intersection between S_1 and S_0 . A dynamics study using a hybrid molecular mechanics with valence bond (MMVB) method shows the nature of the channels leading from this intersection toward the ground state products and indicates that all possible photoproducts are accessible from this conical intersection.

Methodological Details

Ab Initio. The CASSCF *ab initio* computations¹² used an eight electron, eight orbital active space involving the π -orbitals of the benzene and ethene moieties. The geometries were optimized using the 4-31G basis set, and the energies were recomputed at the 6-31G* level. The algorithm used to locate conical intersections on the surface by simultaneously locating an intersection hyperline and minimizing the remaining ($N-2$) geometric variables has been documented elsewhere.¹³

MMVB. The molecular mechanics with valence bond (MMVB) method¹⁴ combines a molecular mechanics (MM2)

force field description of the inactive atoms with a parametrized Heisenberg Hamiltonian¹⁵ valence bond description that represents the active electrons of a CASSCF calculation. The VB part is defined by connections between pairs of valence atoms; currently there are only general VB parameters for sp^2/sp^3 carbon atoms that simulate CASSCF/4-31G energies.¹⁴ Due to the nature of the Heisenberg Hamiltonian only covalent states can be described. With this method, ground and excited state energies and analytical gradients are available for very little computational effort. The algorithm to locate conical intersections¹³ is also available for this procedure. MMVB has been used for hydrocarbons corresponding to CASSCF calculations with 10^{16,17} and 18 active electrons,¹⁸ reproducing very well the *ab initio* results on the ground and excited states.

Dynamics. Direct molecular dynamics calculations¹⁹ have been performed with the MMVB potential just described. The equations of motion are solved using local quadratic approximations²⁰ to the potential surface with a trust radius.²¹ An ensemble of trajectories—a “classical wave packet”—is generated by randomly sampling each excited state normal mode within an energy threshold. The algorithm used to determine where the trajectories hop to the ground state²² depends on both the kinetic energy of the molecule and the energy gap between the states. When the trajectory hops the energy difference between the states is redistributed into the momentum along the direction of the nonadiabatic coupling vector, as suggested by Truhlar.²³

Results

A Simple VB Model for the S_1 Surface Topology. Whilst orbital symmetry arguments are not very helpful in making *a priori* predictions about the structures (Scheme 1) that may be relevant on the S_1 surface for this reaction, a simple VB model (see ref 12a) can be used as we shall now discuss. The lowest energy electronic states of polyenes are essentially covalent, and the minima and other points can be rationalized in terms of VB structures with at least one uncoupled pair of electrons.²⁴ Further, as we have shown in other work, the photochemistry of benzene²⁵ and styrene²⁶ can be understood by considering simple VB structures on the excited state surfaces with two or four partly uncoupled electron pairs. The S_1/S_0 crossing points can also be rationalized in this fashion. Accordingly it is our intention in this section to consider the possible minima and crossing points that may occur on the S_1 surface in terms of simple VB structures.

(11) (a) Bernardi, F.; Olivucci, M.; Robb, M. A. *J. Am. Chem. Soc.* **1992**, *114*, 5805. (b) Rossi, I.; Olivucci, M.; Bernardi, F.; Robb, M. A. *J. Phys. Chem.* **1995**, *99*, 6757.

(12) Gaussian 94; Frisch, M. J.; Trucks, G. W.; Schlegel, H. B.; Gill, P. M. W.; Johnson, B. C.; Robb, M. A.; Cheeseman, J. R.; Keith, T. A.; Petersson, G. A.; Montgomery, J. A.; Raghavachari, K.; Al-Laham, M. A.; Zakrzewski, V. G.; Ortiz, J. V.; Foresman, J. B.; Cioslowski, J.; Stefanov, B. B.; Nanayakkara, A.; Challacombe, M.; Peng, C. Y.; Ayala, P. Y.; Chen, W.; Wong, M. W.; Andres, J. L.; Replogle, E. S.; Gomperts, R.; Martin, R. L.; Fox, D. J.; Binkley, J. S.; Defrees, D. J.; Baker, J.; Stewart, J. P.; Head-Gordon, M.; Gonzalez, C.; Pople, J.; Gaussian, Inc.: Pittsburgh, PA, 1995.

(13) Bearpark, M. J.; Robb, M. A.; Schlegel, H. B. *Chem. Phys. Lett.* **1994**, *223*, 269.

(14) Bernardi, F.; Olivucci, M.; Robb, M. A. *J. Am. Chem. Soc.* **1992**, *114*, 1606.

(15) (a) Anderson, P. W. *Phys. Rev.* **1959**, *115*, 2. (b) Said, M.; Maynau, D.; Malrieu, J.-P.; Bach, M.-A. G. *J. Am. Chem. Soc.* **1984**, *106*, 571. (c) Said, M.; Maynau, D.; Malrieu, J.-P. *J. Am. Chem. Soc.* **1984**, *106*, 580. (d) Durand, P.; Malrieu, J.-P. *Adv. Chem. Phys.* **1987**, *67*, 321.

(16) Bearpark, M. J.; Bernardi, F.; Olivucci, M.; Robb, M. A. *Chem. Phys. Lett.* **1994**, *217*, 513.

(17) Bearpark, M. J.; Bernardi, F.; Clifford, S.; Olivucci, M.; Robb, M. A.; Smith, B. R. *J. Am. Chem. Soc.* **1996**, *118*, 169.

(18) Bearpark, M. J.; Bernardi, F.; Clifford, S.; Olivucci, M.; Robb, M. A.; Vreven, T. *Mol. Phys.* **1996**, in press.

(19) Bearpark, M. J.; Robb, M. A.; Smith, B. R.; Bernardi, F.; Olivucci, M. *Chem. Phys. Lett.* **1995**, *242*, 27.

(20) Helgaker, T.; Uggerud, E.; Jensen, H. J. A. *Chem. Phys. Lett.* **1990**, *173*, 145.

(21) Chen, W.; Hase, W. L.; Schlegel, H. B. *Chem. Phys. Lett.* **1994**, *228*, 436.

(22) (a) Preston, R. K.; Tully, J. C. *J. Chem. Phys.* **1971**, *54*, 4297. (b) Preston, R. K.; Tully, J. C. *J. Chem. Phys.* **1971**, *55*, 562.

(23) Blais, N. C.; Truhlar, D. G.; Mead, C. A. *J. Chem. Phys.* **1988**, *89*, 6204.

(24) Celani, P.; Garavelli, M.; Ottani, S.; Bernardi, F.; Robb, M. A.; Olivucci, M. *J. Am. Chem. Soc.* **1995**, *117*, 11584.

(25) Palmer, I. J.; Ragazos, I. N.; Bernardi, F.; Olivucci, M.; Robb, M. A. *J. Am. Chem. Soc.* **1993**, *115*, 673.

(26) Bearpark, M. J.; Olivucci, M.; Wilsey, S.; Bernardi, F.; Robb, M. A. *J. Am. Chem. Soc.* **1995**, *117*, 6944.

Let us consider possible structures with two or four uncoupled electrons. One may consider first *ortho* and *meta* S_1 structures with fully formed C_1-C_7 and C_2-C_8 or C_3-C_8 σ bonds, shown as **I** and **III** in Scheme 1. In this case the remaining four carbon atoms will adopt a structure that is S_1 butadiene-like **I** or prefulvene-like **III**. Since such minima exist on the butadiene²⁷ (at the CASSCF level) and the benzene²⁵ S_1 surfaces one may expect that such minima can be located for the *ortho* and *meta* reaction paths. The *para* structure **IV** has fully formed C_2-C_3 and C_5-C_6 π bonds on the ground state. The excited state must have these two double bonds partly broken and will be rather high in energy.

Now let us consider possible S_1/S_0 crossing points. We have shown in other work that there is a S_1/S_0 conical intersection in *cis*-butadiene that involves twisting both about the central C-C bond and the terminal methylenes. This structure will have its counterpart on an *ortho* addition path in structure **V** which is twisted about the C_4-C_5 bond. Similarly, in benzene²⁵ we have previously documented a prefulvene like conical intersection with a partial C_4-C_6 cross bond. This same allylic conical intersection also exists in allyl.²⁴ This type of intersection has its counterpart on the *meta* pathway shown as **VIII** in Scheme 1. Finally, the four quasi-unpaired electrons in the *para* intermediate **IV** could be arranged in a similar fashion to those in **VI**, but this would be a very strained structure (although such conical intersections are seen in the cycloaddition of Dewar benzene²⁸).

It remains only to consider possible surface crossings where there are no radical centers created. (The zwitterionic structure **II** falls into this class, but we have not investigated reaction paths involving intermediates of this type, which may be relevant with substituent effects). In the S_1 [$2\pi + 2\pi$] cycloaddition of two ethenes, one encounters a rhomboid conical intersection.²⁹ Such an intersection can be postulated for the *ortho* addition path and is shown as **VI** in Scheme 1. Along the *meta* pathway, one may postulate a structure **VII** in which the C_1-C_7 σ bond and the C_5-C_6 π bond are fully formed leaving four adjacent partly coupled electrons on centers $C_2, C_3, C_4,$ and C_8 . Such a conical intersection has been documented in the but-1-ene sigmatropic rearrangement^{11a} and of the allyl group in hexa-1,5-diene.^{11b}

In summary one can predict, *a priori*, that one may have minima **I** and **III** (and possibly **IV**) with adjacent conical intersections **V** and **VIII** on the *ortho* and *meta* S_1 reaction paths. Alternatively quasi-concerted paths on S_1 may exist that must pass via conical intersections of the form **VI** or **VII**. As we shall now discuss, all these structures do exist on the ethene + benzene S_1 reaction surface. However, as we will show, only **VII** occurs at low energy. The structures with biradical centers will be stabilized by substituent effects and may be relevant in other reactions with radical stabilizing substituents.

Ab initio computations: The results of the CASSCF calculations are shown in Tables 1 and 2. Table 1 shows the CASSCF/4-31G S_0 and S_1 energies along with a cross reference to Figures 2–11 which contain the optimized geometries. The reference point corresponds to the Franck–Condon excitation geometry. Here the energies for both S_0 and S_1 are optimized at the minimized ground state geometry where the benzene and ethene fragments are separated by 10 Å. The CASSCF/6-31G*

Table 1. CASSCF/4-31G Energies and Figures

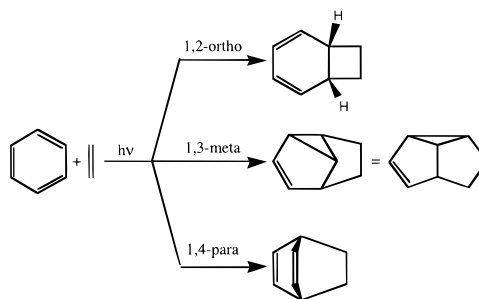
| geometry ^a | state | $E(S_0)^d$ | $E(S_1)^d$ | Figure |
|------------------------------|-------------------|-------------------------------|-------------------|--------|
| <i>ortho</i> product | S_0 | -80.9 | | 3 |
| <i>meta</i> product | S_0 | -73.8 | | 4 |
| <i>para</i> product | S_0 | -91.2 | | 5 |
| I | S_1 | | 39.7 | 6 |
| III | S_1 | | 23.9 | 7 |
| IV | S_1 | | 46.2 | 8 |
| V | S_1/S_0 | 48.7 ^b | 49.0 ^b | 9 |
| VI | S_1/S_0 | 20.1 ^b | 20.3 ^b | 10 |
| VII | S_1/S_0 | -1.3 ^b | -1.1 ^b | 2a |
| VIII | S_1/S_0 | 33.0 ^b | 33.1 ^b | 11 |
| S_0 benzene + S_0 ethene | S_1 and S_0^c | -116.0 | 0 | |
| | | $\Delta E(S_1 - S_0) \hat{=}$ | | |
| | | 246.6 nm | | |

^a In Scheme 1. ^b State averaged orbitals. ^c Full MC-SCF energy minimization for each state, at this geometry. ^d kcal mol⁻¹ relative to the S_1 energy of benzene + ethene at the S_0 geometry (-308.2225 E_h).

Table 2. CASSCF/6-31G* Energies at 4-31G Geometries

| geometry ^a | $E(S_0)^d$ | $E(S_1)^d$ |
|------------------------------|-------------------------------|-------------------------------|
| I | | 29.0 |
| III | | 12.4 |
| IV | | 34.6 |
| V | 34.2 | 36.5 ^b |
| VI | 15.4 | 20.1 ^b |
| VII | -6.0 | -4.6 ^b |
| VIII | 20.7 | 23.0 ^b |
| S_0 benzene + S_0 ethene | -115.6 | $\Delta E(S_1 - S_0) \hat{=}$ |
| | $\Delta E(S_1 - S_0) \hat{=}$ | 247.5 nm |

^a In Scheme 1. ^b State averaged orbitals. ^c Full MC-SCF energy minimization for each state, at this geometry. ^d kcal mol⁻¹ relative to the S_1 energy of benzene + ethene at the S_0 geometry (-308.6525 E_h).

**Figure 1.** Possible reaction products of a model arene + olefin photoreaction.

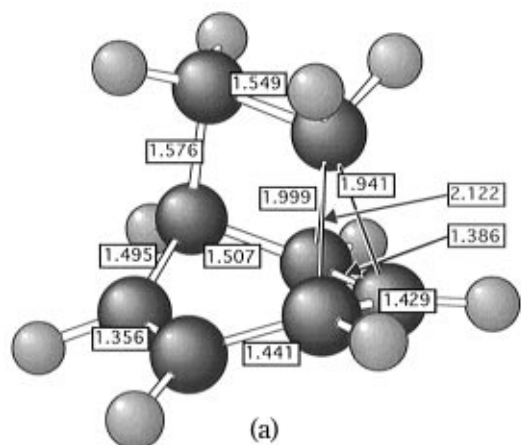
energies of S_0 and S_1 and the relative energies of these excited state structures at the 4-31G geometries are reported in Table 2. Our objective in this work is to document the S_1 surface topology. It is clear that the energies of the S_1/S_0 intersections and minima have the same relative order at the 6-31G* level, and the S_1/S_0 degeneracy remains at this higher level of theory.

From the data presented in Tables 1 and 2 and Figures 2–11 it is clear that *all* the minima **I**, **III**, and **IV**, and the associated S_1/S_0 conical intersections **V**–**VIII** actually exist on the 4-31G potential surface. The only low energy structure is **VII** which is an S_1/S_0 conical intersection. In spite of extensive searches, we can find no transition state along a reaction path leading to this structure. This conical intersection has a geometry (the $C_2-C_3-C_4-C_8$ pyramid) that is similar to the one encountered in the sigmatropic migration of the methyl group in but-1-ene that we have studied previously. Thus for the model ethene plus benzene reaction the formation of the C_1-C_7 bond occurs without barrier to yield a low energy conical intersection. Decay from this point may form either the *ortho*, *meta*, or *para*

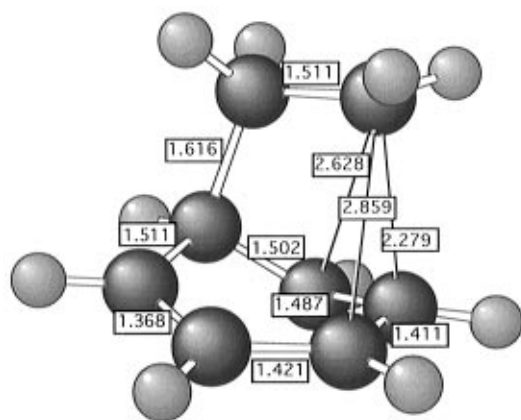
(27) (a) Olivucci, M.; Ragazos, I. N.; Bernardi, F.; Robb, M. A. *J. Am. Chem. Soc.* **1993**, *115*, 3710–3721. (b) Celani, P.; Bernardi, F.; Olivucci, M.; Robb, M. A. *J. Chem. Phys.* **1995**, *102*, 5733.

(28) Bernardi, F.; Olivucci, M.; Palmer, I.; Robb, M. A. *J. Org. Chem.* **1992**, *57*, 5081.

(29) Bernardi, F.; De, S.; Olivucci, M.; Robb, M. A. *J. Am. Chem. Soc.* **1990**, *112*, 1737.



(a)



(b)

Figure 2. MMVB (a) and CASSCF/4-31G geometries for the dynamics conical intersection.

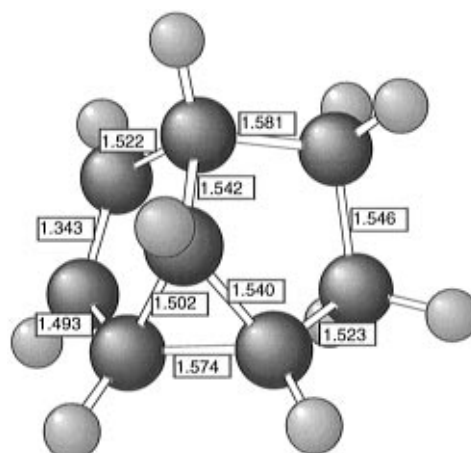


Figure 4. CASSCF/4-31G 1,3-product minimum geometry.

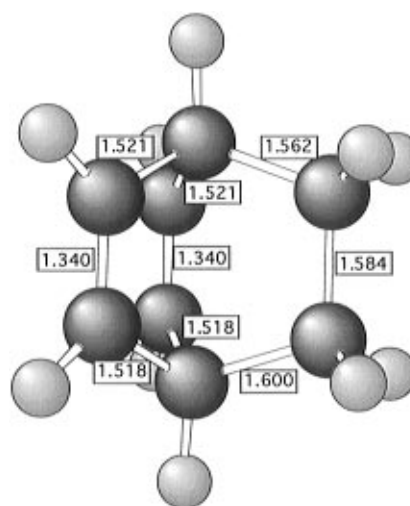


Figure 5. CASSCF/4-31G 1,4-product minimum geometry.

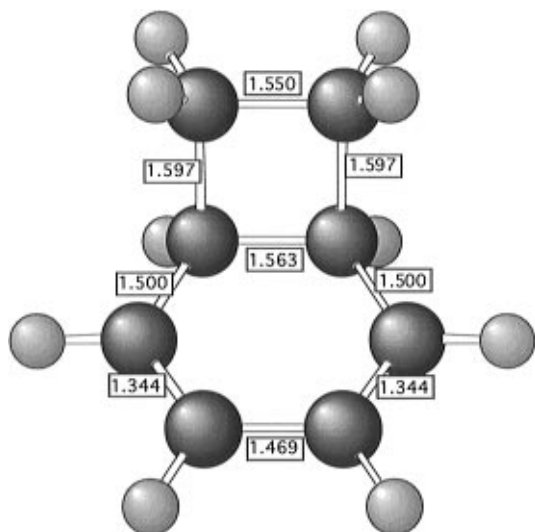


Figure 3. CASSCF/4-31G 1,2-product minimum geometry.

products, and thus the reactivity will be determined by the dynamics of the decay at this point, which we shall discuss subsequently. The fact that the low energy crossing **VII** is reached without barrier is consistent with experiment. In other work²⁵ we have shown that the loss of fluorescence in benzene³⁰ associated with a vibrational excess of 3000 cm^{-1} is due to passage via a transition state through a conical intersection to

(30) Kaplan, L.; Wilzbach, K. E. *J. Am. Chem. Soc.* **1968**, *90*, 3291–3292.

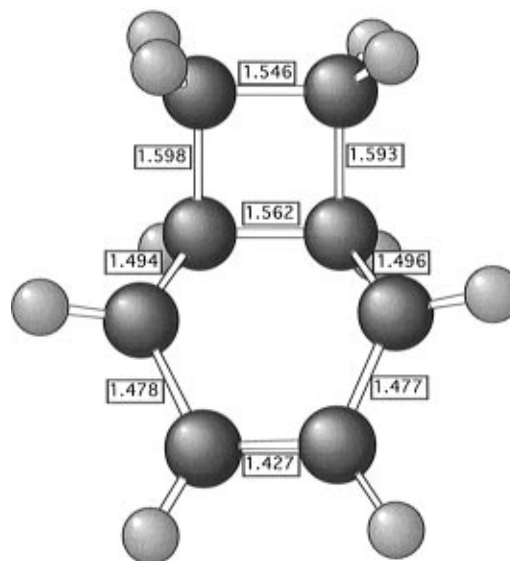


Figure 6. CASSCF/4-31G 1,2-excited state minimum geometry.

prefulvene. The barrier for ethene + benzene cycloaddition must therefore be small or zero to compete effectively with prefulvene formation.

The simple VB model discussed in the previous subsection rationalizes the existence of critical points on S_1 and their approximate energetic ordering. The two lowest energy S_1 conical intersections are those with the least radical character (**VI** and **VII**). The two prefulvene-like structures (**III** and **VIII**)

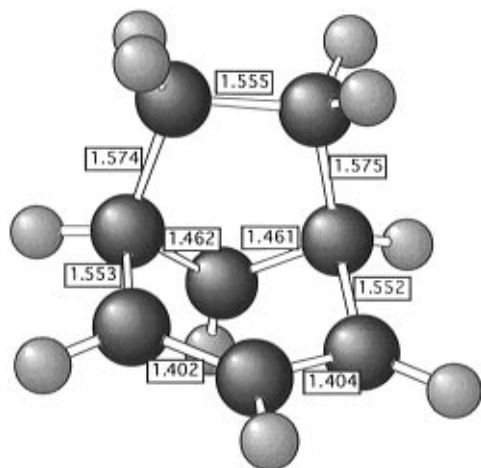


Figure 7. CASSCF/4-31G 1,3-excited state minimum geometry.

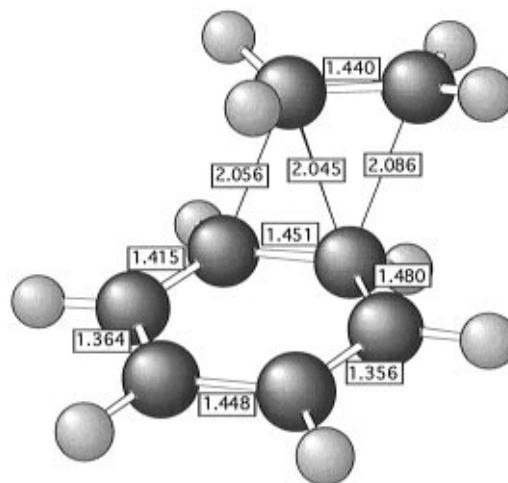


Figure 10. CASSCF/4-31G 1,2-conical intersection geometry.

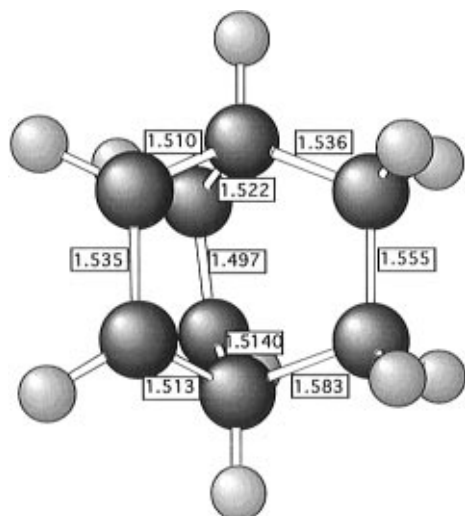


Figure 8. CASSCF/4-31G 1,4-excited state minimum geometry.

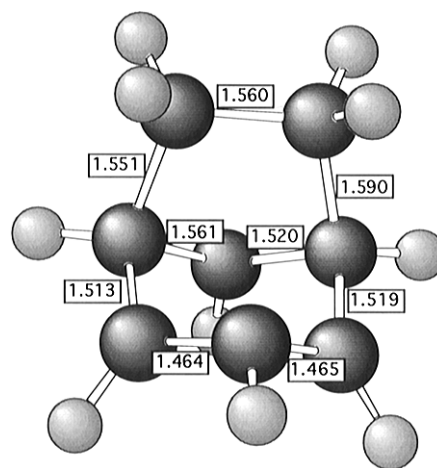


Figure 11. CASSCF/4-31G 1,3-conical intersection geometry.

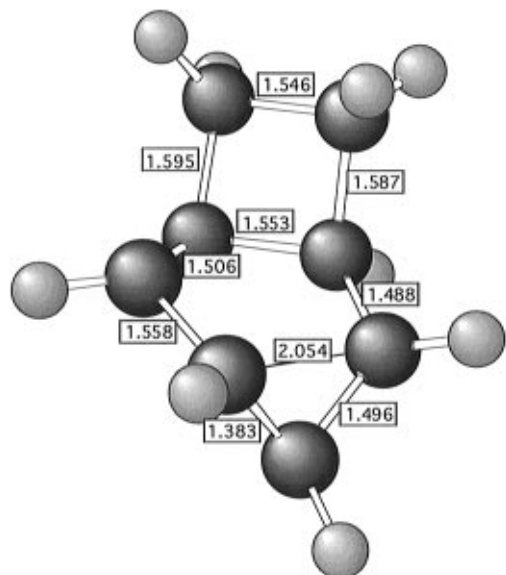


Figure 9. CASSCF/4-31G 1,2-conical intersection geometry.

with one completely uncoupled electron and an allyl-like fragment are next lowest. The two distinctly biradical structures (I and V), and the *para* geometry with broken π bonds (III) are highest.

Substituents that can stabilize the biradical centers C₃ and C₆ of I and V may stabilize these *ortho* intermediates and

crossing points. The structures III and VIII for the *meta* pathway may be stabilized in a similar fashion. Thus the major role of substituents may be to deform the shape of the S_1 potential surface and favor one reaction path. The experimental evidence for the regioselectivity of the *meta* addition clearly indicates that electron donating substituents on the arene are found at positions on the final products that correspond to C₂ and C₅ of the intermediate structure III, whilst electron withdrawing substituents are found at positions that correspond to C₄ and C₆ of III [see ref 2 for summary of *meta* experimental data]. Thus substituted arenes *meta* add to olefins to give products that are consistent with having an intermediate structure like III. The experimental data for the *ortho* addition are much more complicated and seem to indicate that the regioselectivity is probably not governed by any single process, and can depend on a variety of factors, including temperature, solvent polarity, as well as the substituents on the arene.⁷ Therefore we shall not attempt to explain the *ortho* regioselectivity with our simple, unsubstituted model system.

Dynamics Study of the Decay from the Lowest Energy Point on the Conical Intersection. Since the lowest energy point of the conical intersection VII is reached without barrier from the reactants, the product distribution must be controlled by the dynamics of decay through the conical intersection and the population of ground state reaction paths. In previous dynamics studies of the type reported here, the starting point for the computations was either the Franck–Condon region,¹⁷

(31) Bearpark, M. J.; Bernardi, F.; Olivucci, M.; Robb, M. A.; Smith, B. R. *J. Am. Chem. Soc.* **1996**, in press.

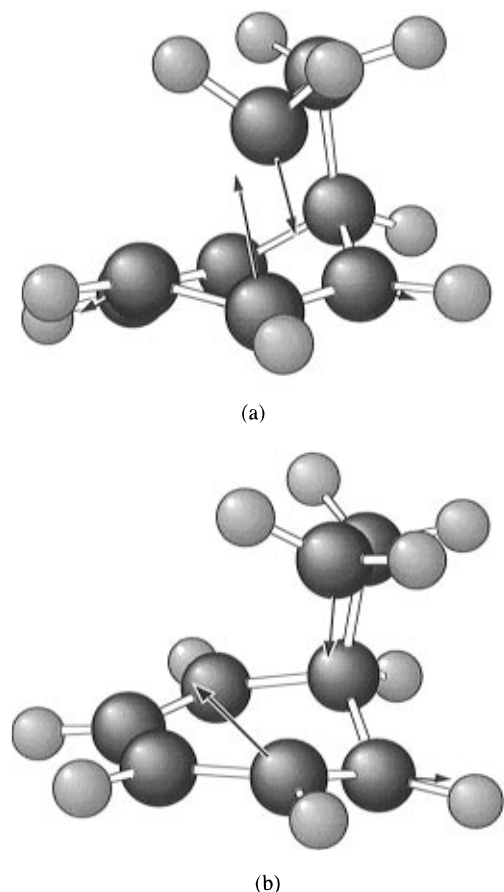


Figure 12. Derivative coupling vectors from MMVB (a) and CASSCF/4-31G (b).

the S_1 minimum³¹ (i.e., 0–0 transition point), or an S_1 transition state.¹⁹ Even at high excess energies, the surface hop always occurred close to the geometry corresponding to the lowest point on the conical intersection. Accordingly, the region near the minimum energy point on the conical intersection has been used as the starting point of our dynamics computations since we are interested in ground state product distributions.

Dynamics computations at the CASSCF level are presently not feasible. Accordingly for the dynamics study we have used the MMVB potential described in the computational details section. Although, we cannot expect quantitative results with this approach, a qualitative picture of the factors controlling product formation can be obtained.

The MMVB and CASSCF geometries of the conical intersection **VII** are shown in Figure 2. The general nature (i.e., the benzene ring) of the structures optimized with each method is similar. However the size of the C₂–C₃–C₄–C₈ pyramid is significantly smaller in the MMVB structure. The degeneracy associated with a conical intersection is lifted by motion in the plane defined by the gradient difference vector and the direction of the nonadiabatic coupling vector. The most important aspects of the dynamics must be controlled by the nature of this plane. Here the CASSCF and MMVB nonadiabatic coupling (Figure 12) and gradient difference (Figure 13) vectors for this conical intersection (**VII**) are in good agreement.

As a prelude to our discussion of the dynamics, one may gain insight into the nature of the ground state potential surface near conical intersection **VII** using the concept of a steepest descent line (i.e., trajectories where the kinetic energy is set to zero at each step and thus correspond to a steepest descent path in mass weighted coordinates). We have followed ground state steepest descent lines (SDL) from 12 equally spaced geometries

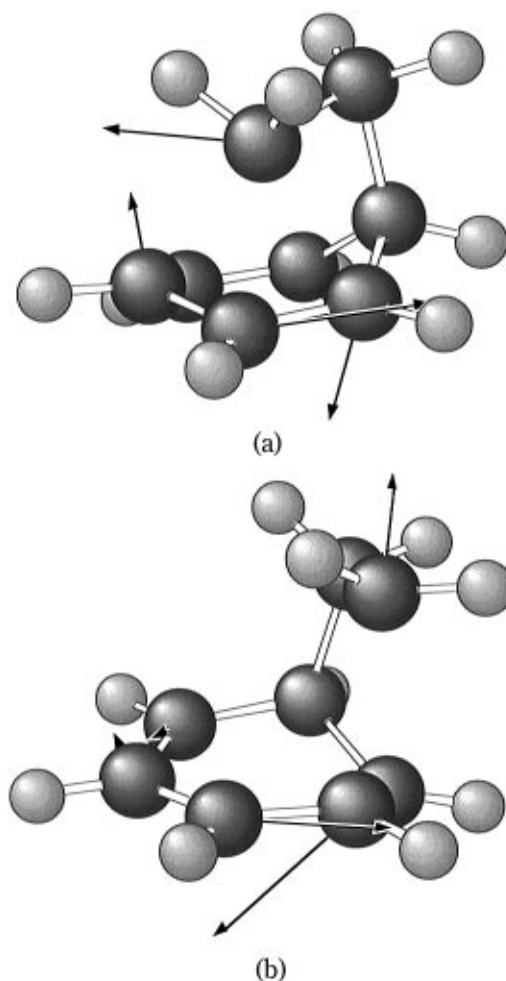


Figure 13. Gradient difference vectors from MMVB (a) and CASSCF/4-31G (b).

around a “circle” (of radius 0.02 Å) centered on the conical intersection (**VII** in Scheme 1, Figure 2a). The circle corresponds to distortions only in the plane of the two degeneracy lifting coordinates. To illustrate the motion of the atoms as one passes around the circle the geometries are shown superimposed upon one another with a common center of mass in Figure 14 (the displacements in this Figure are scaled by a factor of 3 for clarity).

The termination points of the 12 SDL are reported in Table 3. These clearly show that there exists a channel (300° to 0° in Table 3) leading to the 1,3 *meta* product in the direction of gradient difference vector (0° in Table 3). SDL from the intersection in all other directions terminate at the 1,2 *ortho* product. SDL to dissociation and the 1,4 *para* product are not seen at all. This implies that the *meta* product formation channel is narrower and less deep than the *ortho*. However, this is simply a reflection of the greater stability of the S_0 *ortho* minimum. We do not find an SDL leading to the *para* product from our searches in the branching plane. Thus SDL leading to this structure, if they exist at all, must begin outside the branching plane.

The starting point of our excited state dynamics study was also 12 equally spaced geometries around the same “circle” (with a larger radius of 0.1 Å) centered on the same conical intersection (**VII** in Scheme 1, Figure 2a). The radius of the circle is chosen such that the starting points are between 21 and 42 kcal mol⁻¹ above the intersection. From each of these points an ensemble of 64 trajectories was generated by randomly sampling each excited state normal mode within an energy

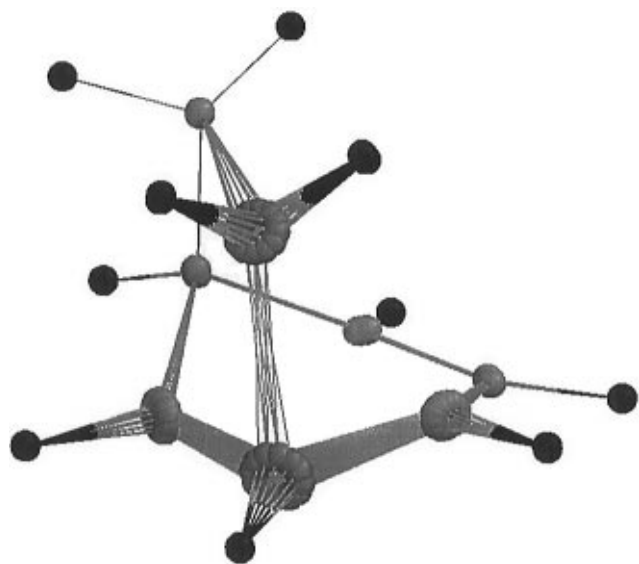


Figure 14. Schematic representation of the "circle" centered (corresponding to distortions in the plane of the two degeneracy lifting coordinates) on the conical intersection (**VII** in Scheme 1, Figure 2a). The displacements in this Figure are scaled by a factor of 3 for clarity.

Table 3. Termination Points of Steepest Descent Line Calculations

| SDL | angle (deg) | product formed | SDL | angle (deg) | product formed |
|-----|-------------|----------------|-----|-------------|----------------|
| 1 | 0 | 1,3 | 7 | 180 | 1,2 |
| 2 | 30 | 1,2 | 8 | 210 | 1,2 |
| 3 | 60 | 1,2 | 9 | 240 | 1,2 |
| 4 | 90 | 1,2 | 10 | 270 | 1,2 |
| 5 | 120 | 1,2 | 11 | 300 | 1,3 |
| 6 | 150 | 1,2 | 12 | 330 | 1,3 |

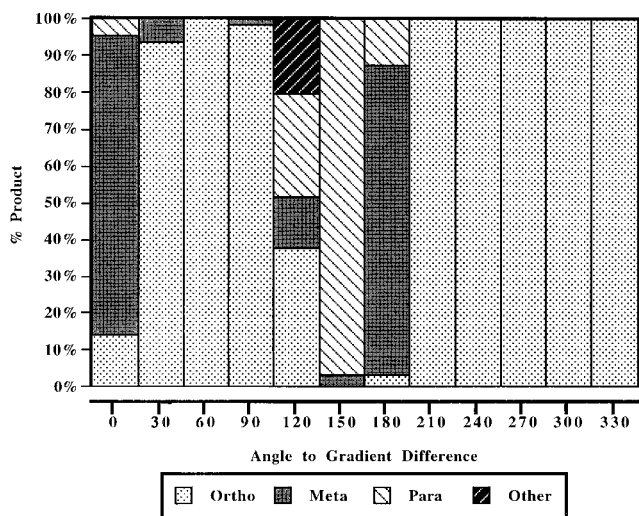


Figure 15. Fractional yield of products from the trajectories plotted against the angle of the ensemble reference geometries to the gradient difference vector Figure 13.

threshold with an average range of 11 kcal mol⁻¹. Our objective is to obtain a statistical view of the product ratios that can be correlated with the direction in which the system approaches the intersection on the excited state. The result of each trajectory consists of the final geometry and the final electronic state. The possible outcomes are the *ortho*, *meta*, and *para* ground state products and trajectories where the ethene and benzene fragments are well separated on *S*₀ corresponding to dissociation.

In our dynamics simulation, all trajectories hopped immediately from *S*₁ to *S*₀ which is consistent with the fact that

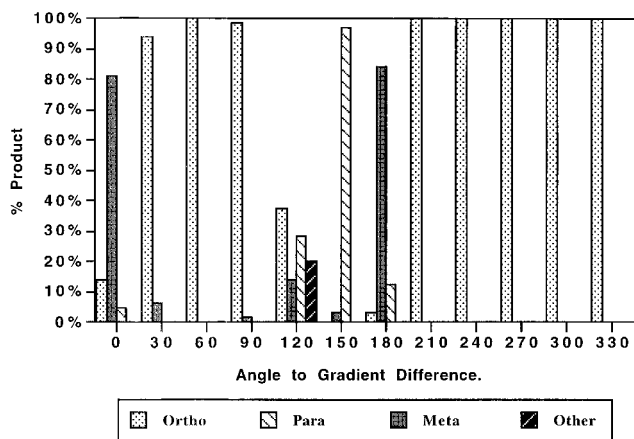


Figure 16. Percent yield of products of trajectories plotted against the angle of the ensemble reference geometries to the gradient difference vector Figure 13.

the conical intersection is the lowest energy point on the *S*₁ surface. Figures 15 and 16 illustrate the outcomes of the trajectories plotted against the angle of the ensemble reference geometries to one of the defining coordinates of the plane—in this case the gradient difference vector. The results yield similar conclusions to those from the SDL study. The *meta* product only forms from ensembles entering the funnel along the gradient difference vector (0° and 180°), as do the *para* and dissociation products. Note that the *meta* product is seen at 180° in the dynamics simulation but not in the SDL study because the 180° trajectory "reverses" immediately after the hop. The *ortho* product is generated by trajectories that enter the intersection outside of the narrow band that characterizes the *meta* product.

The dynamics results show virtually no new effects that are not qualitatively obvious from the nature of the conical intersection itself and the nature of the ground state reaction paths that we computed with the SDL approach. The only dynamic feature relates to the fact that one sees the production of the *para* product even though there is no SDL that leads to this structure. Obviously, since most experiments are carried out in solution where the system can lose kinetic energy quickly, the *para*-type trajectories may fall into the *meta* "channel". However, the *para* path involves a large rearrangement of the atoms in the benzene moiety toward a quinoid structure, and the starting points for trajectories to this product may not lie on the branching plane (i.e., not along the circle that we have used).

Conclusion

For the model ethene + benzene photocycloaddition, experimental results from 1977² show that the ratio of the *meta* adduct to *ortho* product (or its photoproducts) is approximately equal. From the exhaustive compilation of Cornelisse,² it appears that for many arene + olefin systems one or both of the 1,2- and 1,3-cycloadditions proceed with good yields, whereas the 1,4-addition is a less efficient process preferred only by a few special cases. While various excited state intermediates have been postulated, there has been no experimental evidence that has proved the existence of any long-lived intermediate.

The central result of our study demonstrates the existence of a low energy conical intersection (**VII** in Scheme 1) that can be reached from the reactants without barrier. SDL and dynamics studies in the region of this intersection show that trajectories can lead to all the of photochemical products observed. Whilst various higher energy biradical minima (some

with adjacent conical intersections) can be optimized on the potential surface, all the photoproducts can be rationalized in terms of decay from the single low energy crossing **VII**. We therefore suggest that the major role of substituent effects may be to move this central conical intersection closer to the *ortho* or *meta* side by stabilising the incipient biradical structures such as **V** or **VIII**.

Acknowledgment. This research has been supported in part by the SERC (UK) under Grants GR/J25123 and GR/H58070 and by Gaussian Inc. through a studentship for S. Clifford. All

ab initio computations were run on an IBM RS/6000 using a development version of the Gaussian 94 program.¹² MMVB computations were run on a Cray T3D at the Parallel Computing Centre, University of Edinburgh (EPCC).

Supporting Information Available: Tables S1 and S2 CASSCF/4-31G energies and CASSCF/6-31G* energies in atomic units (hartrees) (2 pages). See any current masthead page for ordering and Internet access instructions.

JA961078B